JOURNAL OF Materials Chemistry Communication

Crystal structure of the ferromagnetic superconductor $RuSr_2(Gd_{1.3}Ce_{0.7})Cu_2O_{10-\delta}$ by powder neutron diffraction

Christopher S. Knee, Brian D. Rainford and Mark T. Weller*

Department of Chemistry and Department of Physics, University of Southampton, Highfield, Southampton, UK SO17 1BJ. E-mail: mtw@soton.ac.uk

Received 28th July 2000, Accepted 31st August 2000
First published as an Advance Article on the web 19th September 2000

The 1222-type ferromagnetic, superconducting cuprate, $RuSr_2(^{160}Gd_{1.3}Ce_{0.7})Cu_2O_{10-\delta}$, contains RuO_6 octahedra that are rotated 13.4° around the *c*-axis and tilted reducing the Cu–O(1)–Ru angle to 168.2° at 295 K. The oxygen deficiency δ has been determined as 0.22, indicating a hole doping mechanism, similar to that proposed for $GdSr_2RuCu_2O_8$, facilitates superconductivity.

The tripled-perovskite structure family represents one of the most important series of superconducting cuprates, which includes the widely studied $YBa_2Cu_3O_{7-\delta}$.[1] Recently, one member of this system, $RuSr_2GdCu_2O_8$ (Ru-1212), has been the focus of new attention since the demonstration of the extremely unusual coexistence of ferromagnetism and bulk superconductivity within the material.[2–4] Felner *et al.*[5] have reported similar equally remarkable magnetic behaviour for the structurally related phase $RuSr_2(Gd_{1.4}Ce_{0.6})Cu_2O_{10-\delta}$ (Ru-1222), establishing transition temperatures for bulk superconductivity, $T_c = 42$ K, and magnetic order $T_M = 180$ K compared with $T_c = 35$ K and $T_M = 133$ K for $RuSr_2GdCu_2O_8$.[6] The layered structures of these compounds play a vital role in allowing the coexistence of the two phenomena, minimising pair-breaking effects as carrier momentum and field are aligned parallel to the *xy*-plane. However, recent neutron diffraction experiments on Ru-1212 have shown the magnetic order is predominately antiferromagnetic,[7] implying a canted spin arrangement allowing both ferro- and antiferromagnetic components. Supporting evidence for this scenario is provided by crystallographic results on $RuSr_2GdCu_2O_8$ that have revealed localised distortions of the RuO_6 octahedra.[6,8] Detailed structural information is therefore paramount for understanding the ability of the ruthenium cuprates to support two apparently conflicting magnetic phenomena.

This communication reports the results of a structural study performed using powder neutron diffraction (PND) on $RuSr_2(^{160}Gd_{1.3}Ce_{0.7})Cu_2O_{10-\delta}$. The structure may be related to that of $RuSr_2GdCu_2O_8$ by inserting a fluorite type $(Gd_{1+x},Ce_{1-x})O_2$ block in place of the single Gd layer, shifting alternate perovskite blocks by $(a+b)/2$, Fig. 1. PND has allowed the key metal–oxygen coordination to be accurately resolved, the oxygen deficiency δ to be determined and the temperature dependence of the structure to be monitored.

A 1.5 g polycrystalline sample of $RuSr_2(^{160}Gd_{1.3}Ce_{0.7})Cu_2O_{10-\delta}$ was prepared *via* solid state reaction of high-purity reagents RuO_2, CuO, $Sr(NO_3)_2$, CeO_2 and $^{160}Gd_2O_3$ following the literature method,[9] with an additional final annealing step at 1100 °C for a further 48 h and slow cooling to room temperature. The use of ^{160}Gd is necessary to avoid the strong neutron absorption of natural gadolinium. Phase purity monitored using powder X-ray diffraction revealed a small ($\sim$5%) but persistent level of the impurity Sr_2GdRuO_6. The magnetic properties of this sample were probed using an Oxford instruments VSM to reveal a $T_c \approx 29$ K, while the deviation between ZFC and FC curves, which indicates ferromagnetic ordering, occurs initially near $T_M \approx 180$ K with the main deviation at 90 K; these values are similar to those reported previously for this material.[5] PND data were collected at 10 K and 295 K, on the high-resolution diffractometer D2B at the I.L.L. operating with $\lambda = 1.594$ Å, and an acquisition time of 8 hours.

Rietveld analysis[10] of the 10 K data commenced using the literature model.[9] Introduction of atomic and thermal parameters revealed an unacceptably large temperature factor ($B_{iso} = 10.1(3)$ Å^2) for the O(3) oxygen that links the ruthenium centres indicating structural disorder. This atom was therefore displaced from the original 4c (0,½,0) site to a 50% occupied 8j (0.12,½,0) position and subsequent refinement produced a reasonable temperature factor and significantly improved fit statistics. A slight reduction in the overall occupancy of this split site was also found on refinement. Introduction of an anisotropic temperature factor for the apical to ruthenium oxygen (O(1)) revealed seemingly significant horizontal thermal disorder ($B_{11} = B_{22} = 1.98(6)$, $B_{33} = 0.48(7)$ Å^2) incompatible with the low temperature of data collection. The scattering from this site was therefore modelled by displacing the atom along *x* to give a quarter occupied 16n (*x*,0,*z*) $x \sim z \sim 0.05$ site, that refined to produce realistic positional and thermal parameters.

The good contrast in neutron scattering lengths between the cations, *e.g.* $^{160}Gd = 9.50$, $Sr = 7.02$ and $Ce = 4.84$ fm,[11] permitted the refinement of the site occupancies for the individual metal cations. For the Gd/Ce and Sr sites any deviation from the expected cation distribution was too small to significantly improve the fit and the site occupancies were therefore fixed at their initial values. The copper and ruthenium site occupancies also refined to within 1% of full occupancy. The occupancies of the other oxygen sites were probed and the O(4) oxygen, which lies in the centre of the fluorite block, was the only one to show a statistically significant ($>3\sigma$) decrease. Finally, the small

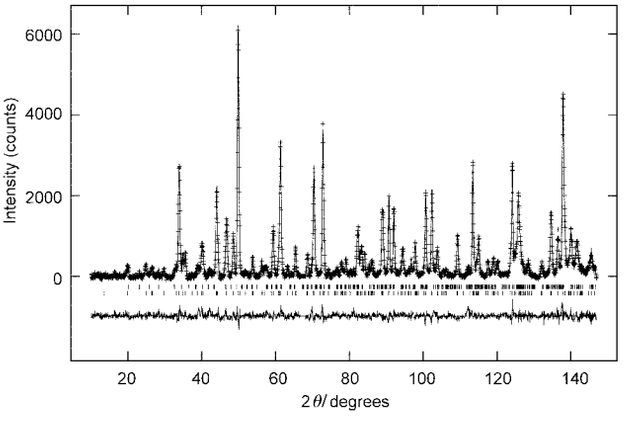

Fig. 1 Rietveld fit for $RuSr_2(^{160}Gd_{1.3}Ce_{0.7})Cu_2O_{10-\delta}$ at 10 K. Allowed reflections positions are indicated with tick marks for Ru-1222 (lower) and Sr_2GdRuO_6 (upper).

DOI: 10.1039/b006120o

Table 1 Refined structural parameters for $RuSr_2(^{160}Gd_{1.3}Ce_{0.7})Cu_2O_{10-\delta}$ at 10 and 295 K (upper and, where different, lower values respectively). Space group *I*4/*mmm*

T/K	*a*/Å	*c*/Å	R_{wp} (%)	R_p (%)	χ^2
10	3.83382(3)	28.5213(5)	4.42	3.40	1.73
295	3.84237(10)	28.5803(9)	3.75	2.80	1.81

Atom	Site	*x*	*y*	*z*	B_{iso}/Å^2	*n*
Gd/Ce	4e	½	½	0.2049(1)	0.46(4)	0.65/0.35
				0.2049(1)	0.80(4)	
Sr	4e	½	½	0.0779(1)	0.42(5)	1.0
				0.0776(1)	0.99(5)	
Cu	4e	0	0	0.1439(1)	0.38(3)	1.0
				0.1440(1)	0.61(3)	
Ru	2a	0	0	0	0.49(6)	1.0
					0.72(7)	
O(1)	16n	0.041(2)	0	0.0673(1)	0.6(1)	0.25
		0.052(3)		0.0670(1)	0.6(1)	
O(2)	8g	0	½	0.15012(8)	0.65(4)	1.0
				0.15038(7)	0.96(4)	
O(3)	8j	0.124(1)	½	0	1.1(1)	0.48(1)
		0.119(1)		0	1.3(1)	0.47(1)
O(4)	4d	0	½	¼	0.43(7)	0.94(2)
				¼	0.69(8)	0.93(1)

impurity Sr_2GdRuO_6 was fitted and the crystal fraction refined to 3%, a level too small to have detectable implications for the stoichiometry of the main phase.

The same refinement procedure was followed for the 295 K data. Refined structural parameters for both temperatures are summarised in Table 1 and derived interatomic distances and angles listed in Table 2. The final profile fit achieved (10 K data) is shown in Fig. 1.

The refined displacements of the basal and apical oxygens of the RuO_6 are critical to the interpretation of the magnetic behaviour of Ru-1222 (Fig. 2), and analogous disorder has been reported for $RuSr_2GdCu_2O_8$.[6,8] Importantly, the low temperature refinement confirms that the disorder is static in nature rather than a result of lattice motion. The displacement of O(3) by $\sim$0.5 Å in the *xy*-plane corresponds to a rotation of the RuO_6 octahedra by 13.4° about the *c*-axis at room temperature, slightly less than that observed for Ru-1212 by Chmaissem *et al.* using PND.[6] The origin of the disorder is the size mismatch between the Ru–O and Cu–O layers and displacement of O(3) allows the in-plane Ru–O bond to achieve a physically reasonable value of $\sim$1.975(1) Å. Our data reveal no evidence of supercell reflections arising from extended regions of correlated RuO_6 rotations in contrast to the data from $RuSr_2{}^{160}GdCu_2O_8$.[6] The smaller displacement of the apical O(1) atom represents a tilt of the octahedra that reduces the Ru–O–Cu angle to 168.2° at 295 K, slightly less than the value of 169.9° determined from a synchrotron X-ray study of Ru-1212.[8]

A small contraction of the Cu–O(2) in-plane distance occurs upon cooling while the Ru–O(3) bond remains constant, indicating an increase in bond mismatch that is alleviated by greater rotation of the RuO_6 octahedra at 10 K. The biggest change occurs for the apical Cu–O(1) interaction which shrinks by $\sim$0.02 Å while the Ru–O(1) distance stays at 1.925 ± 0.001 Å. This behaviour is subtly different from that reported for $RuSr_2{}^{160}GdCu_2O_8$ in which the apical Cu–O(1) bond length decreases by a similar amount while the Ru–O(1) apical bond exhibits negative thermal expansion leaving the vertical Cu–Ru separation effectively unchanged. The difference may reflect a structural change associated with the Ru ordering within Ru-1222, or may simply be a consequence of the split O(1) site introduced in our structural model in contrast to the anisotropic temperature factor employed by Chmaissem *et al.*[6] To check this the results of the refinements with an anisotropic thermal parameter in place of the split position were analysed. These showed that the Cu–O(1) distance still decreased by 0.02 Å, however, the Ru–O(1) bond now

Table 2 Interatomic distances (Å) and bond angles (°) in $RuSr_2(^{160}Gd_{1.3}Ce_{0.7})Cu_2O_{10-\delta}$ at 10 and 295 K

Bond	10 K	295 K
Gd/Ce–O(2) ×4	2.473(2)	2.474(2)
Gd/Ce–O(4) ×4	2.308(2)	2.313(2)
Sr–O(3) ×2	2.649(3)	2.657(4)
Sr–O(3) ×2	3.266(4)	3.253(4)
Sr–O(2) ×4	2.813(3)	2.831(3)
Sr–O(1) ×2	2.620(7)	2.589(5)
Sr–O(1) ×2	2.841(8)	2.887(6)
Cu–O(1) ×1	2.190(5)	2.213(4)
Cu–O(2) ×4	1.9251(3)	1.9298(3)
Ru–O(1) ×2	1.926(3)	1.925(3)
Ru–O(3) ×4	1.975(1)	1.975(1)
O(1)–Cu–O(2)	91.2–99.4(3)	89.9–100.9(2)
O(2)–Cu–O(2)	169.4(2)	169.2(2)
Cu–O(1)–Ru	171.2(6)	168.2(4)
Ru–O(3)–Ru	152.2(2)	153.2(2)

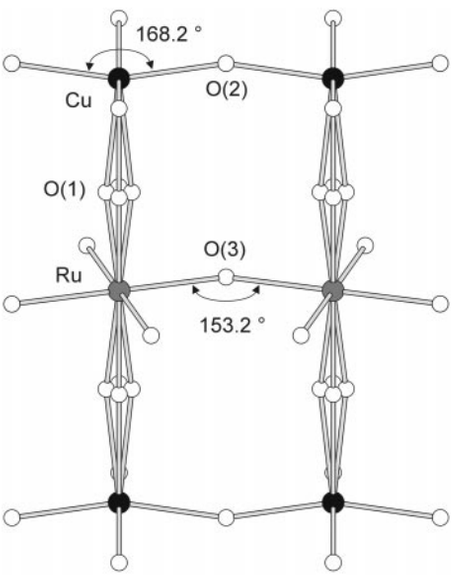

Fig. 2 The disordered Ru–O and Cu–O coordination within $RuSr_2(^{160}Gd_{1.3}Ce_{0.7})Cu_2O_{10-\delta}$.

increased slightly upon cooling resulting in a smaller but still significant decrease in the Cu–Ru separation of 0.014 Å.

The refined stoichiometry from the 295 K data of $RuSr_2(^{160}Gd_{1.3}Ce_{0.7})Cu_2O_{9.78}$ reveals a small level of oxygen deficiency despite the lengthy oxygen anneals employed in the synthesis. The oxygen vacancies are located on the O(4) site of the fluorite $(Gd,Ce)O_{2-x}$ block and on the disordered RuO_2 basal site O(3) (Table 1). If all the ruthenium present adopts a +5 oxidation state this would yield a copper oxidation state of $\sim +2.0$, analogous to stoichiometric $RuSr_2GdCu_2O_8$. This implies a similar hole doping mechanism arising from overlap of the Ru: t_{2g} and the Cu: $d_{x^2-y^2}$ bands is responsible for superconductivity in $RuSr_2(^{160}Gd_{1.3}Ce_{0.7})Cu_2O_{9.78}$ rather than, as previously thought, a direct result of the charge balance necessitated by the separating $(Gd_{1.3},Ce_{0.7})O_2$ fluorite block. Bond valence calculations indicate a Cu oxidation state of $\sim +2.4$, calculated using the 295 K bond lengths and the method of ref. 12. For a conventional high T_c cuprate this would lie in the overdoped region and no superconducting transition would be expected. A copper oxidation state of +2.4 would require a ruthenium valence $\sim +4$ for charge neutrality, *i.e.* the same valence as obtained for the ferromagnet $SrRuO_3$,[13] and consistent with the ferromagnetic order detected for the phase.

The significant oxygen disorder within the Ru–O coordination provides experimental evidence to support the interpretation of Felner *et al.*[5] that localised distortions of the RuO_6 lead to antisymmetric exchange coupling of a Dzyaloshinsky–Moriya type between neighbouring Ru spins to produce canting and net moment within Ru-1222. The full temperature dependence of the structure of the compound and further results on the correlated magnetic behaviour will be presented in a full paper.[14] Preliminary analysis has failed to reveal any additional magnetic intensity arising from ordering of the Ru spins at 10 K.

Acknowledgements

We thank the EPSRC for grant GR/M21836 in aid of this work and the I.L.L for provision of neutron facilities.

Notes and references

1 M. K. Wu, J. R. Ashburn, C. J. Torng, R. L. Meng, L. Gao, Z. J. Huang, Y. Q. Wang and C. W. Chu, *Phys. Rev. Lett.*, 1987, **58**, 909.
2 L. Bauernfeind, W. Widder and H. F. Braun, *Physica C*, 1995, **254**, 151.
3 J. L. Tallon, C. Bernhard, M. E. Bowden, P. W. Gilberd, T. M. Stoto and D. J. Pringle, *IEEE Trans. Appl. Supercond.*, 1999, **9**, 1696.
4 C. Bernhard, J. L. Tallon, C. Niedermayer, Th. Blasius, A. Golnik, E. Brucher, R. K. Kremer, D. R. Noakes, C. E. Stronach and E. J. Ansaldo, *Phys. Rev. B*, 1998, **59**, 14099.
5 I. Felner, U. Asaf, Y. Levi and O. Milo, *Phys. Rev. B*, 1997, **55**, R3374.
6 O. Chmaissem, J. D. Jorgensen, H. Shaked, P. Dollar and J. L. Tallon, *Phys. Rev. B*, 2000, **61**, 6401.
7 J. W. Lynn, B. Keimer, C. Ulrich, C. Bernhard and J. L. Tallon, *Phys. Rev. B*, 2000, **61**, R14965.
8 A. C. Mclaughin, W. Zhou, J. P. Attfield, A. N. Fitch and J. L. Tallon, *Phys. Rev. B*, 1999, **60**, 7512.
9 K. B. Tang, Y. T. Qian, Y. D. Zhao, L. Yang, C. Zuyao and Y. H. Zhang, *Physica C*, 1996, **259**, 168.
10 A. C. Larson and R. B. Von Dreele, General Structure Analysis System, Los Alamos National Laboratory, LAUR86-748, 1994.
11 L. Koester, H. Rauch and E. Seymann, *At. Data Nucl. Data Tables*, 1991, **49**, 65.
12 J. L. Tallon, *Physica C*, 1990, **168**, 85; J. L. Tallon, *Physica C*, 1995, **176**, 547.
13 L. Klein, J. S. Dodge, C. H. Ahn, J. W. Reiner, L. Mieville, T. H. Geballe, M. R. Beasley and A. Kapitulnik, *J. Phys.: Condens. Matter*, 1996, **8**, 10111.
14 C. S. Knee and M. T. Weller, manuscript in preparation.